KINETIC AND THERMODYNAMIC STUDIES ON ADSORPTION BEHAVIOUR OF RHODAMINE B DYE ON NOSEAN SYNTHESISED FROM COAL FLY ASH.

[1]Sanjay R. Kankrej, [2]Mayuri S. Kulkarni, [3]Rajendra P. Patil, [4]Ashok V. Borhade
[1] Associate professor in Chemistry, [2]Assistant professor in Chemistry, [3] Associate professor in Chemistry,
[4]Associate professor in Chemistry
[1]Department of Chemistry,
[1]Bhonsala Military College, Nashik - 422005, India.

ABSTRACT

Release of colouring agents like Rhodamine B dye in water bodies is an important environmental problem as it is carcinogenic and non-bio-degradable. On the other hand plethora of coal fly ash (CFA) produced in thermal power stations is another threat to the environment. Considering these problems; present study deals with recyclability and modification of waste coal fly ash into alumino-silicate Nosean [$Na_8Al_6Si_6O_{24}(SO_4).H_2O$] by fusing CFA with alkali at 550 ^{0}C followed by hydrothermal treatment. The synthesised nosean was fully characterized by FT-IR, XRD, SEM and BET surface area and it was further checked for potential application for removal of the dye Rhodamine B from its aqueous solutions using batch method. The obtained equilibrium data were fitted by the Langmuir, Freundlich, and Temkin and Dubinin-Radushkevich isotherm models. The well-known thermodynamic parameters such as change in Gibb's free energy (ΔG), entropy change (ΔS) and enthalpy change (ΔH) were evaluated first time for nosean to check the possibility of adsorption process. Further the kinetic parameters such as rate constant and order of adsorption process is also estimated.

Index Terms- Fly ash, hydrothermal, Nosean, adsorption, Rhodamine B.

I. INTRODUCTION

In the current era various dyes are used in textile industry to dye fibre viz. methylene blue, acid violet, erioglaucine, Rhodamine B, etc. The discharge of these colouring agents into water creates serious environmental issues because of non-degradable and toxic nature of these dyes [1]. The surface as well as underground water gets contaminated creating grave environmental problems and health hazards [2]. Rhodamine B dye is one of the valuable dye used in textile industries. Medically it is proved that Rhodamine B is carcinogenic [3]. Drinking water contaminated by Rhodamine B dye could cause tissue borne sarcoma which ultimately causes cancer. Therefore, it is necessary to remove the dye from wastewater before it is discharged to the environment.

From last 20 to 30 years many workers developed various methods for removal of dyes including electrochemical technique [4], biological process [5] and physical process like adsorption. Now a days, number of adsorbents are used for adsorption including duolite C-20 resin [6], exhausted coffee ground from water [7], walnut shells [8], activated carbon and rice husk [9], casuarina equisetifolia needles (CEN) [10]; however their adsorption capacities are very much less, therefore new adsorbents are being discovered. In present study alumino-silicate nosean is used as adsorbent, which is synthesized from coal fly ash (CFA) by alkali fusion followed by hydrothermal process.

All over the world nearly 500 million tonnes of coal fly ash is produced every year by burning coal in thermal power stations to generate the electricity. The demand of electricity is increasing day by day and therefore the amount of coal fly ash produced will also increase in future. Coal fly ash is used for preparation of various products including bricks, cement and concrete [11]. Coal fly ash is rich in SiO_2 and Al_2O_3 content therefore it can be easily transformed in to different zeolites. Many worker have reported on synthesis of different types of zeolites from fly ash [12-38].

Moreover, the recyclability and modification of coal fly ash into zeolitic materials is the best and environmental friendly way of utilization of CFA. Although several studies have been reported in literature on the synthesis of different zeolites using fly ash but reports are not available on synthesis of nosean from fly ash and its potential application for removal of Rhodamine B dye from aqueous medium.

Nosean is a mineral of the sodalite group having formula $Na_8Al_6Si_6O_{24}(SO_4)$. It forms isometric crystals of variable colour – white, grey, blue and green to brown. Nosean possess a typical lattice structure consisting of cages of 12 tetrahedron AlO_4 or similar unit and 12 tetrahedral SiO_4 unit and similar 5 units linked together by oxygen bridges in an alternating pattern to

form truncated octahedron with 8 single 6 ring 3 opening and 6 single 4 rings typically the cage has unit cell parameter (a^0) of 6.6 ^{0}A.

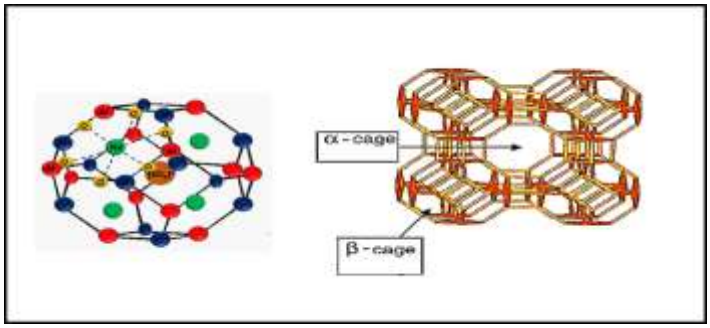

Fig.1: Structure of Nosean showing α and β cages

This paper first time reports the synthesis of aluminosilicate nosean from CFA, its characterization and potential application for removal of Rhodamine B dye from aqueous solution. This study allow us to verify Langmuir, Freundlich, Temkin and Dubinin-Radushkevich adsorption isotherms along with thermodynamic and kinetic studies.

II. EXPERIMENTAL

2.1 Chemicals and materials

Analytical grade chemicals were used without any further purification. Sodium hydroxide, NaOH with ≥ 98.5 wt. % purity, Sodium Sulphate, $Na_2(SO_4)$ purity of ≥ 99.9 wt. %, , Rhodamine B , of purity ≥ 97% wt. were obtained from Sigma Aldrich. Sample of coal fly ash (CFA) was obtained from Eklahara Thermal Power Plant, Nashik (India).

2.2 Nosean synthesis

Before the use of CFA its quantitative chemical composition was determined by inductively coupled plasma (ICP) spectroscopy (Table-1).

Table 1: Chemical composition of raw coal fly ash

Constituents	Na_2O	Al_2O_3	SiO_2	K_2O	CaO	Fe_2O_3	MgO	OtherLOI
Weight/ %	00.23	29.03	55.00	01.38	02.52	07.36	00.80	03.68

From the ICP data, the [SiO_2/Al_2O_3] ratio is found to ≈ 1.89, hence CFA is the best source of aluminium and silicon for the synthesis of nosean. However; to improve the chemical composition, raw CFA was sieved and Fe_2O_3 was removed by magnetic separation. The raw CFA is repeatedly washed with distilled water and dried in the oven at 120 ^{0}C for 24 h. 15 g. of the treated CFA was mixed with equal quantity of NaOH and fused in a silica crucible at 550 ^{0}C for 2 h. This fused mass was cooled, milled and mixed with 150 ml distilled water and then 90 g. Na_2SO_4 was added slowly with constant stirring. This reaction mixture was transferred into Teflon lined stainless steel autoclave (250 ml capacity). The autoclave was kept at 100 ^{0}C for 144 h. The polycrystalline yellowish white product obtained was filtered and washed repeatedly to remove excess NaOH and Na_2SO_4. Further the same product was dried at 120 ^{0}C in the oven for 24 h and heated at 550 ^{0}C in a furnace for 2 h. The obtained product was characterized and used for its potential application for the removal of Rhodamine B dye from its aqueous solution.

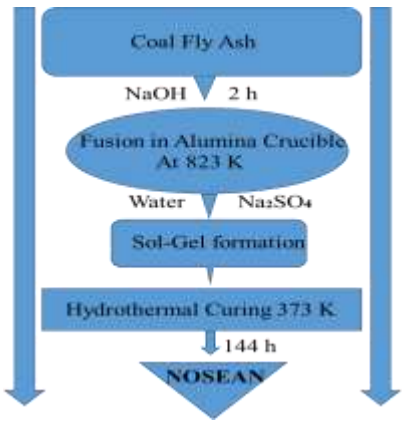

Fig. 2: Flow-sheet for hydrothermal synthesis of nosean using coal fly ash

2.3 Characterization of nosean

Fourier transform infrared (FT-IR) absorption spectra of coal fly ash and hydrothermally prepared nosean was recorded on Shimadzu 8400: S FT-IR Spectrophotometer using KBr pellets in the range of (4000 to 400 cm^{-1}). The phase purity can be identified in unmodified coal fly ash , nosean and nosean after adsorption of Rhodamine B dye was analysed by X-ray powder diffraction pattern using Philips PW-1710 instrument operating at 25 kV and 25 mA using Cu Kα radiation with wavelength λ = 0.154 nm. To provide the information about the surface morphology scanning electron microscopy (SEM) analysis were carried out with the help of JEOL-JEM-6360A model equipment JEOL-JEC-560 auto carbon coater. The BET surface area of nosean was determined by Autosorb-1 NOVA – 1200.

2.4 Batch sorption experiment

Different adsorption isotherms were verified using batch sorption method. Various parameters such as effect of time, initial concentration of dye and dose were studied by measuring the absorbance of the filtrate at 554 nm (λ_{max} of Rhodamine B dye) by using UV-Visible spectrophotometer.

2.4.1 Effect of concentration of Rhodamine B dye

The concentrations ranging from 1 to 6 ppm of Rhodamine B dye solution were prepared from the stock solution by appropriate dilutions using double distilled water. 25 ml of these dye solutions of different concentrations were taken in a series of glass stoppered bottles, 0.100 g nosean was then added to each bottle. These bottles were maintained at desired constant temperature for 3 h and shaken manually at frequent time intervals. After 3 h the solutions were filtered through Whatmann filter paper. The filtrate was then analysed by measuring the absorbance of the filtrate at 554 nm (λ_{max} of Rhodamine B dye) using UV-Visible spectrophotometer.

2.4.2 Effect of contact time

25 ml of Rhodamine B dye solution of predetermined optimum concentration (4 ppm) was taken in a series of glass stoppered bottles. Then 0.020 g of nosean was added in each bottle. These bottles were maintained at desired constant temperature and shaken manually at frequent intervals and then filtered through Whatmann filter paper at various time intervals (from 1 to 70 min). The filtrate obtained was then analysed by measuring the absorbance of the filtrate at 554 nm (λ_{max} of Rhodamine B dye) using UV-Visible spectrophotometer.

2.4.3 Effect of dose variation

25 ml solutions of 4 ppm concentration of Rhodamine B dye were taken in a series of glass stoppered bottles. Different amount (0.005, 0.010, 0.015, 0.020, 0.025, 0.030, and 0.035) g of nosean were added to these bottles. These bottles were maintained at desired constant temperature for 3 h and shaken well. After 3 h the solutions were filtered through Whatmann filter paper and filtrates thus obtained were analysed by the same method as discussed in 2.4.1.

The amount adsorbed at equilibrium (Q_e, $mg.g^{-1}$) was calculated by using the formula reported by Vanderborght and Van Griekenm[39],

$$Q_e = \frac{(C_0 - C_e)V}{m} \quad \text{.....(1)}$$

Where, C_0 and C_e ($mg.L^{-1}$) are the liquid-phase concentration of Rhodamine B at initial and equilibrium respectively, V is the volume of solution (L) and m is the mass of the adsorbent (g).

III. DATA ANALYSIS

3.1 Langmuir adsorption isotherm

Langmuir adsorption isotherm postulates formation of monolayer on the surface of adsorbent. This isotherm also postulates uniform energies of adsorption and also finite number of identical sites on the surface of adsorbent [40]. The linear form of the expression derived by Langmuir and is represented as

$$\frac{1}{Q_e} = \frac{1}{Q_0} + \frac{1}{K_L Q_0 C_e} \quad \text{.....(2)}$$

where, Q_e ($mg.g^{-1}$) is the amount of adsorbate, C_e ($mg.L^{-1}$) is the concentration of adsorbate at equilibrium, Q_0 ($mg.g^{-1}$) is the maximum monolayer coverage capacity, and K_L ($L.mg^{-1}$) is the equilibrium adsorption constant or Langmuir isotherm constant which is related to the affinity of the binding sites. The values of K_L and Q_0 were calculated from the slope and intercept [41]. The important feature of this isotherm is the equilibrium parameter or separation factor R_L, which is a dimensionless entity and is given by [42].

$$R_L = \frac{1}{1 + K_L C_0} \quad \text{.....(3)}$$

Where, C_0 is the initial concentration, R_L value indicated the feasibility of adsorption process, If $0 < R_L < 1$ adsorption is favourable, If $R_L = 1$ adsorption is linear, if $R_L > 1$ adsorption is unfavourable and if $R_L = 0$ then adsorption process is irreversible.

3.2 Freundlich adsorption isotherm

The linear form of Freundlich adsorption isotherm can be expressed as –

$$\log Q_e = \log K_f + \frac{1}{n} \log C_e \quad \text{.....(4)}$$

Where, Q_e ($mg.g^{-1}$) and C_e ($mg.L^{-1}$), are having the same significance as above, K_f ($mg.g^{-1}$) and (1/n) are Freundlich constants related to the adsorption capacity and strength of adsorption or intensity of adsorption respectively [43]. If n = 1, then partition

between the two phases are independent of the concentration. If value of 1/n < 1, it indicates the normal adsorption and if 1/n > 1, then it indicates that the adsorption is cooperative adsorption [44]. If n is between 1 and 10, indicates adsorption process is a favourable process [45].

3.3 Temkin isotherm

This model assumes that heat of adsorption (which is the function of temperature) of all molecules in the layer would decrease linearly rather than logarithmic with coverage [46, 47]. The model is given by the following equation,

$$Q_e = \frac{RT}{b_T}\ln A_T + \frac{RT}{b_T}\ln C_e \quad \text{……..(5)}$$

If $B = \frac{RT}{b_T}$, then,

$$Q_e = B\ln A_T + B\ln C_e \quad \text{……..(6)}$$

where, A_T is Temkin isotherm equilibrium binding constant ($L.g^{-1}$), b_T is Temkin isotherm constant, R is universal gas constant (8.314 $kJ.mol^{-1}.K^{-1}$), T is absolute temperature and B is the constant related to heat of sorption ($J.mol^{-1}$). The smaller value of B indicates physical sorption and larger value shows chemical sorption.

3.4 Dubinin-Radushkevich isotherm

This isotherm is mainly applied to express the mechanism of adsorption with Gaussian energy distribution onto a heterogeneous surface [48, 49]. The expression for this isotherm is given as-

$$Q_e = (Q_s)\exp(-K_{ad}\,\mathcal{E}^2) \quad \text{……..(7)}$$

The linear from of the above equation is,

$$\ln Q_e = \ln Q_s - K_{ad}\,\mathcal{E}^2 \quad \text{……..(8)}$$

Where, Q_e, ($mg.g^{-1}$) is the amount of adsorbate adsorbed by the adsorbent at equilibrium, Q_s , ($mg.g^{-1}$) is the theoretical isotherm saturation capacity, K_{ad} , ($mol^2.kJ^{-2}$ is the Dubinin-Radushkevich isotherm constant) and ε is the potential energy; which can be calculated as,

$$\mathcal{E} = RT\ln[1 + (1/C_e)] \quad \text{……..(9)}$$

Where, R is gas constant (8.314 $J.mol^{-1}$), T is the absolute temperature and C_e represents equilibrium concentration of adsorbate ($mg.L^{-1}$). When ln(Q_e) is plotted verses square of the potential energy ε^2 , a straight line with the slope = K_{ad} and intercept = ln (Q_s) will be obtained.

The mean free energy E is related to the K_{ad}; the Dubinin-Radushkevich isotherm constant as;

$$E = [1/\sqrt{2K_{ad}}\,] \quad \text{……..(10)}$$

Low value of E, mean free path energy indicates the physisorption process.

3.5 Thermodynamic studies:

The thermodynamic feasibility for adsorption process is checked by, the thermodynamic parameters, such as change in Gibb's free energy (ΔG) , enthalpy change (ΔH) and entropy change (ΔS) were evaluated using equation (11) and (12),

$$-RT\ln K_a = \Delta G \quad \text{……..(11)}$$

$$\Delta H - T\,\Delta S = \Delta G \quad \text{……..(12)}$$

Substituting eq. (12) in eq. (11), we get

$$\frac{\Delta S}{R} - \frac{\Delta H}{RT} = \ln K_a \quad \text{……..(13)}$$

Where, K_a is the thermodynamic distribution coefficient for the adsorption and is calculated by using eq. (14)

$$K_a = \frac{C_a}{C_e} \quad \text{……..(14)}$$

Where, C_a, ($mg.g^{-1}$) is the concentration of metal ion adsorbed by absorbent and C_e , ($mg.L^{-1}$) is the equilibrium concentration of metal ion, R is the gas constant (8.134 $J.mol^{-1}.K^{-1}$) and T is the temperature in Kelvin (K).

3.6 Kinetic studies

The adsorption kinetic parameters of sorption process of Rhodamine B dye on the adsorbent nosean, the extent of sorption is studied for contact time ranging from 1 - 70 min. by estimating the percentage removal of Rhodamine B dye. The kinetic data were analysed by using pseudo-first-order, pseudo-second-order, Intra-particle diffusion model and Bangham's equation.

3.6.1 The pseudo-first-order model [50]

The appropriate values of the pseudo-first-order rate constant, k_1, are obtained by the model represented as-

$$\log(Q_e - Q_t) = log\,(Q_e) - \frac{k_1\,t}{2.303} \quad \text{……..(15)}$$

Where, Q_t, ($mg.g^{-1}$) is amount of adsorbate adsorbed at time 't', Q_e, ($mg.g^{-1}$) the adsorption capacity at equilibrium, k_1 (min^{-1}) is the pseudo-first-order rate constant and t (min) is the contact time. The values of the adsorption rate constant, k_1 for Rhodamine B dye were determined from the plot of log (Q_e – Q_t) against 't'.

3.6.2 The pseudo-second-order model [51]

This model is represented by the equation,

$$\frac{t}{Q_t} = \frac{1}{k_2\,(Qe)^2} + \frac{1}{Qe}\,t \qquad \text{.....(16)}$$

Where, k_2, (g.mg^{-1}. min^{-1}) is the pseudo second order rate constant. The initial adsorption rate h_0, (mg.g^{-1}.min^{-1}) at t = 0 is defined as follows,

$$h_0 = k_2\,(Q_e)^2 \qquad \text{.....(17)}$$

When (t/ Q_t) is plotted versus time, the slope = 1/Q_e and intercept = 1/h_0. Since Q_e is known from the slope, k_2 can be determined from the value of h_0 [52].

3.6.3 The intra-particle diffusion model [53]

The intra-particle diffusion model, which is based on the assumption that adsorption occurs in several steps is represented as film or external diffusion, pore diffusion, surface diffusion and adsorption on the pore surface. The linear form of this model is-

$$Q_t = k_t\,t^{1/2} + C \qquad \text{.....(18)}$$

Where, k_t (mg.g^{-1}.min$^{-1/2}$) is the intra-particle diffusion rate constant and C is the intercept. The value of C relates to the thickness of the boundary layer. The larger C implies the greater effect of the boundary layer [54]. If the plot of Q_t versus $t^{0.5}$ gives a straight line, the adsorption process is controlled by intra-particle diffusion only. However, if the data exhibit multi-linear plots, then two or more steps influence the sorption process. [55]

3.6.4 Bangham's model [56]

To check whether pore diffusion is the only rate controlling step in the adsorption Bangham's model is applied. It is represented by,

$$log\left(\frac{C_0}{(C_0 - mQ_t)}\right) = log\,\frac{(k_b m)}{(2.303\,V)} + \alpha\log(t) \qquad \text{.....(19)}$$

Where, V, (mL) is the volume of solution, and α (< 1) and k_0 are constants. Q_t, (mg.g^{-1}) is the metal uptake per unit weight of adsorbent at time t, Q_e (mg.g^{-1}) is the metal uptake per unit weight of adsorbent at equilibrium. If the experimental data fits in this equation, the adsorption kinetics are limited to the pore diffusion.

IV. RESULT AND DISCUSSION

4.1 FT- IR analysis

The FT-IR spectrum of CFA in Fig. 2(a) shows three wide absorption bands. The peak observed at 1045 cm^{-1} is associated with T-O asymmetric stretching vibrations and may be attributed to the presence of quartz. The bands corresponding to 800 and 557 cm^{-1} can correspond to quartz and mullite respectively present in fly ash. The band at 420 cm^{-1} is associated with T-O bending vibrations [57]. The FT-IR spectrum recorded for hydrothermally synthesized nosean is shown in Fig. 2 (b). Mainly three frequencies are observed in this spectrum; υ_{as} (Al-O-Si) –Asymmetric stretching vibrations ~ 1000 cm^{-1} , υ_s (Al-O-Si) – Symmetric stretching vibrations ~ 750-650 cm^{-1} and δ (O-T-O) – bending vibrations ~ 450-400 cm^{-1} . The shoulder peak at 1123 cm^{-1} is due to symmetric stretching of SO_4 group, the small sharp peak at ~ 637 cm^{-1} and 615 cm^{-1} is due to asymmetric bending vibrations of SO_4 group [58] and absorption band at 3600 cm^{-1} is due to –OH stretching of H_2O molecule. The FT-IR spectrum of hydrothermally synthesised nosean Fig 2 (b) is totally different than the FT-IR spectrum of coal fly ash Fig. 2 (a) clearly confirms the formation of alumino-silicate nosean.

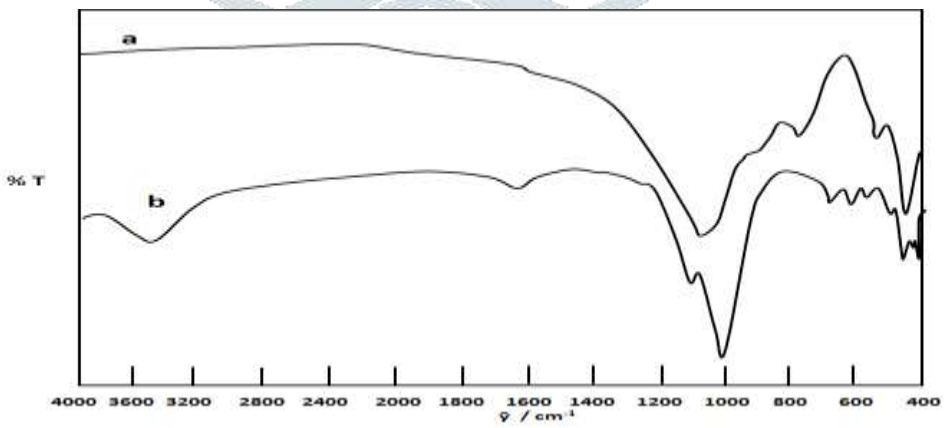

Fig. 2: FT-IR of (a) Coal fly ash and (b) Nosean

4.2 X-Ray powder diffraction analysis

The X-ray powder diffraction pattern of coal fly ash is shown in Fig.3 (a), which mainly shows a broad hump between 20- 30^0 2θ is due to amorphous phase of coal fly ash. Few, very weak peaks are showing the presence of quartz (SiO_2) and mullite ($Al_6Si_2O_{13}$). After fusion, grinding and hydrothermal process several sharp peaks, which corresponds to formation of alumino-silicate nosean are obtained and is shown in Fig. 3 (b). The original peaks because of quartz and mullite are absent in the

X-ray diffraction pattern of nosean. The difference in the X-ray diffraction pattern of coal fly ash and hydrothermally synthesized product confirms the formation of nosean.

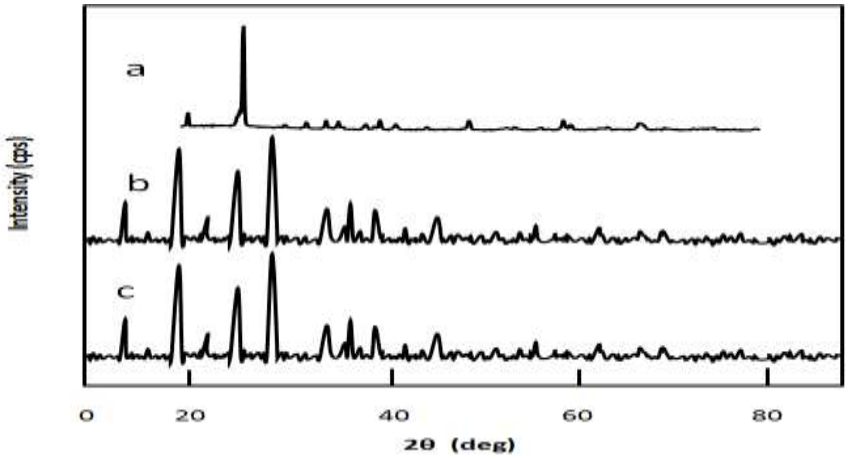

Fig. 3: XRD pattern of (a) Coal fly ash, (b) Nosean and (c) Dye adsorbed nosean.

4.3 SEM analysis

A careful observation of SEM image (Fig. 4 (a)) of coal fly ash shows that most of fly ash particles are spherical in shape with smooth surface. The fusion of coal fly ash with NaOH followed by hydrothermal synthesis of nosean shows clearly the change in the surface morphology from spherical to rod like structure confirms the formation of nosean. (Fig. 4 (b)). Whereas Figure 4 (c) shows nosean after adsorption of Rhodamine B dye and it clearly shows that after adsorption structure of nosean remains unaffected.

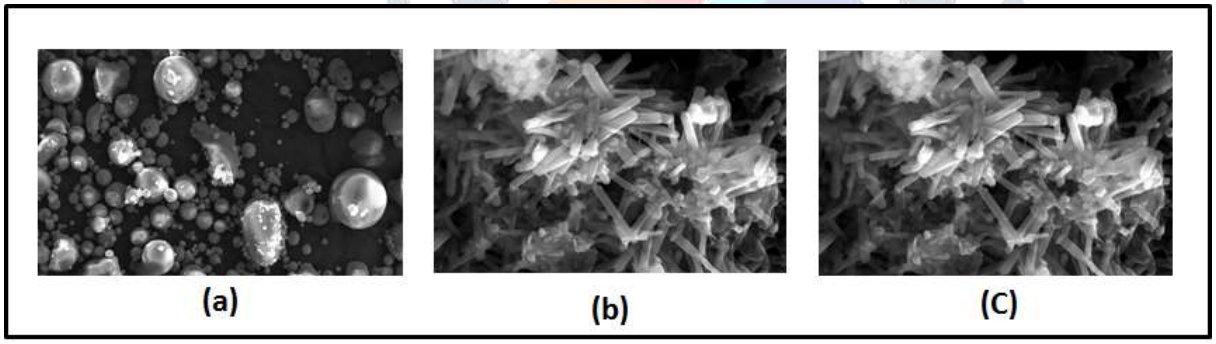

Fig. 4. SEM immages of (a) Coal fly ash , (b) Nosean and (c) Dye adsorbed nosean.

4.4 BET surface area analysis

The BET surface area measurement curve for nosean is represented in Fig. 5. The N_2 adsorption / desorption isotherm and BJH pore size distribution of nosean shows that it has typical IV N_2 adsorption / desorption isotherms with H_1 hysteresis which indicates that the sample serves the spherical mesopores. Based on the isotherms, the specific surface area obtained from BET method is 62.024 $m^2.g^{-1}$ and BJH pore volume is 0.462 cc/g and radius Dv(r) = 87.341 ^{0}A.

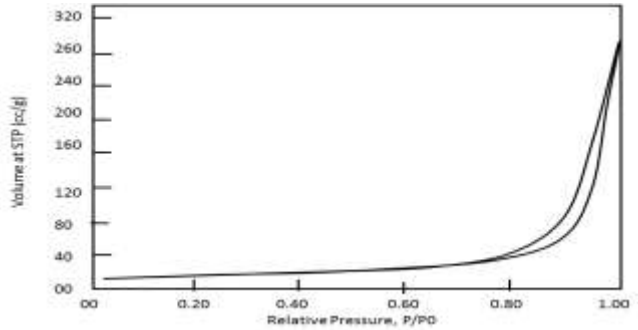

Fig. 5. B-E-T surface area measurement for nosean.

4.5 Effect of contact time

The effect of contact time for the removal of Rhodamine B dye onto nosean is depicted in Fig. 6(a). The adsorption rate was found rapid in the beginning, reaches to maximum and then gradually decreases up to 60 min. The rapid rate of adsorption in the first minute may be due to concentration gradient between adsorbate and number of vacant sites onto the nosean (adsorbent). From Fig. 6 (a) it is clear that the equilibrium is reached a maximum at around 20 min.

4.6 Effect of initial concentration of Rhodamine B dye

To study the effect of concentration of Rhodamine B dye on nosean, dye solution of varying concentrations were used and other parameters like adsorbent dose and contact time were kept constant. (Adsorbent dose was 0.100 gm / 25 ml with contact time 3 h). Figure 6 (b) represents plots of % adsorption as a function of initial concentration of dye solution, and it reveals that, with increase in the initial concentration of Rhodamine B dye solution, the uptake of all the metal ions onto the hydrothermally synthesized nosean also increases up to certain initial concentration of dye and then remains constant. Further in the same figure plateau shows unavailability of the surface and pores for further sorption of dye molecules. After plateau, further increase in the initial concentration of Rhodamine B dye the % adsorption decreases, this may be due to the crowd of dye molecules near the pores of nosean might be decreasing the rate of sorption.

When an adsorbent comes in contact with a Rhodamine B molecules, the concentration of Rhodamine B molecules on the surface of the adsorbent will increase until a dynamic equilibrium is reached, at this point, there is clearly defined distribution of dye molecules between the solid and liquid phases. Rhodamine B dye concentration ranges from (0.1 to 100) $mg.L^{-1}$ with the fixed adsorbent mass. With an increase in dye concentration the removal efficiency increased initially, reaches to maximum value and further decreases with increase in concentration of Rhodamine B dye. It is well known that a given mass of adsorbent material has a definite number of adsorption sites, and with dye concentration, these sites gets saturated. There is a particular dye concentration that shows maximum adsorption for a given adsorbent mass and thereafter, by increasing concentration of dye extent of adsorption cannot increase because no more sites are available on the surface of adsorbent as all sites on the surface of adsorbent are occupied.

4.7 Effect of dose (amount of adsorbent)

To study the effect of dose, varying amount of nosean was added to the series of bottles containing 100 ml of 100 ppm solutions of Rhodamine B dye. The time of contact is kept constant (3 h) for each bottle. Fig. 6(c) shows the % adsorption as a function of dose of absorbent. It was found that, the removal of dye by adsorbent nosean increases with an increases in the adsorbent dose initially and thereafter, becomes constant after some amount of adsorbent weight (W). The increase in extent of adsorption with adsorbent dose can be attributed to the availability of greater surface area and large number of adsorption sites. Whereas with increase in temperature the dye removal decreases due to desorption of dye molecules from the surface of adsorbent.

4.8 Effect of temperature

The effect of temperature on the time dependence of the adsorption process of Rhodamine B dye on hydrothermally prepared nosean was studied at different temperatures (Room temperature, 50 ^{0}C and 75 ^{0}C) by batch experiments. It has been found that % adsorption decreases with increasing temperature. This decrease may be due the adsorption of dye molecules on the surface of nosean only. Here there is no sorption process taking place, as the molecules of dye might not be entering the void of the nosean because of large size of the Rhodamine B dye molecules. With increase in temperature kinetic energy of the dye molecules increases and it gets desorbed from the surface. The thermodynamic study also shows positive slope of the line when ln K is plotted versus 1/T, showing exothermic nature of the adsorption process.

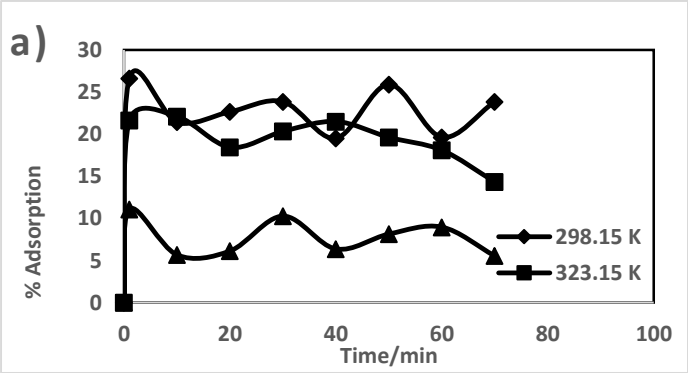

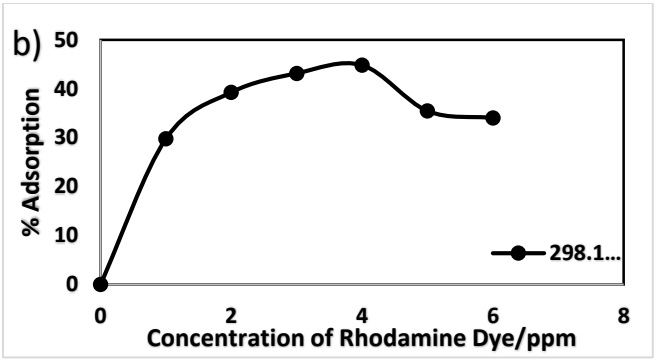

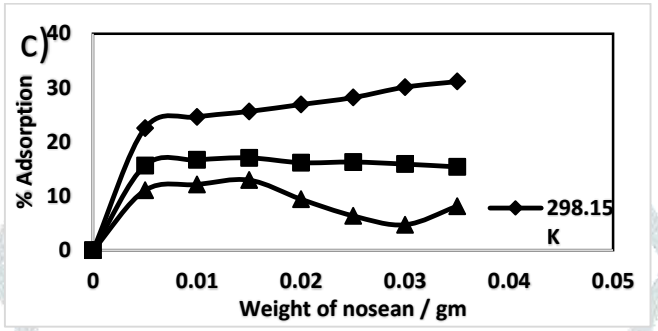

Fig. 6: Effect of (a) Contact time, (b) Concentration of Rhodamine B dye solution and (c) Dose of adsorbent (nosean) on the extent of adsorption at different temperatures.

4.9 Adsorption isotherms

The adsorption data obtained was tested using four most widely used adsorption isotherms viz. Langmuir, Freundlich, Temkin and Dubinin-Radushkevich adsorption isotherms eq. (1), (3), (5) and (8) respectively. The applicability of the adsorption isotherm to the present study was estimated by comparing the values of correlation coefficient (R^2) and other relevant constants.

4.9.1 Langmuir isotherm

Figure 7(a) shows Langmuir plot for adsorption of Rhodamine B dye on nosean. Langmuir constant Q_0, K_L and R_L were calculated using equation (1) and (2). Q_0 indicates the maximum monolayer coverage capacity ($mg.g^{-1}$), K_L is the Langmuir isotherm constant ($L.mg^{-1}$) which also indicates the energy of adsorption, R_L value indicates feasibility of the adsorption, unfavourable (if $R_L > 1$), linear (if $R_L = 1$), favourable (if $0 < R_L < 1$) and irreversible (if $R_L = 0$). From the data presented in Table-2**,** R_L values obtained for adsorption of Rhodamine B dye on nosean are greater than 0 and less than 1 indicating that Langmuir isotherm is favourable for adsorption of Rhodamine B dye on nosean. The Q_0 values decreases with increase in temperature indicates that the adsorption capacity decreased with increasing temperature. This is because of increasing kinetic energy of the adsorbate molecules, which increases the frequency of collisions between the adsorbent and dye molecules and thus gets desorbed from the surface of adsorbent. The Q_0 value for Rhodamine B dye is 3.5894 $mg.g^{-1}$ for nosean. Also by applying linear form of Langmuir equation the mean of correlation factor R^2 value is found to be 0.9713 ± 0.0254 reveals that adsorption data fit well into the adsorption model. The potential applicability of the number of micro- and meso-porous zeolites and other materials are reported by different workers, but nosean shows remarkable adsorption capacity as compared to other adsorbents reported in literature and their results are compared in Table 3.

4.9.2. Freundlich Isotherm

Freundlich adsorption isotherm is illustrated in Figure 7(b) and the corresponding calculated data is presented in Table 2**.** Freundlich model was applied for adsorption of Rhodamine B dye on nosean. Freundlich constants K_f and n calculated using equation (3). The constant K_f is an approximate indicator of adsorption capacity, while 1/n is a function of the strength of adsorption in the adsorption process. Here $1/n > 1$ it indicates that the adsorption is cooperative adsorption. The mean of correlation factor values R^2 is 0.9598 ± 0.0418.

4.9.3. Temkin isotherm

Temkin model was applied for adsorption of Rhodamine B dye on nosean and depicted in Fig. 7 (c) and the data obtained is presented in Table 4. B value is calculated using equation (5) and (6). The plot between the graph of Q_e Versus $\ln(C_e)$, gives, the slope = B ($J.mol^{-1}$) , the small value of B indicates physical sorption and larger value indicates chemical sorption. B values obtained for adsorption at 25, 50 and 75 ^{0}C are 0.6661 $kJ.mol^{-1}$, 2.960 $kJ.mol^{-1}$, and 1.598 $kJ.mol^{-1}$ respectively. All these values are small indicates physical sorption. Also the mean of correlation factor values R^2 is 0.9036 ± 0.1088.

4.9.4 Dubinin-Radushkevich isotherm

Dubinin-Radushkevich model was applied for adsorption of Rhodamine B dye on nosean and is shown in Fig. 7(d). E and Q_s values are calculated using equations (8), (9) and (10) and are listed in Table 4. The plot between ln Q_e versus ε^2, gives, the slope = B ($J.mol^{-1}$), the small value of E (ranging from $4.17x10^{-3}$ $kJ.mol^{-1}$ to $9.37x10^{-3}$ $kJ.mol^{-1}$) giving evidence for physical sorption. The average R^2 value for this model is found to be 0.9526 ± 0.0516.

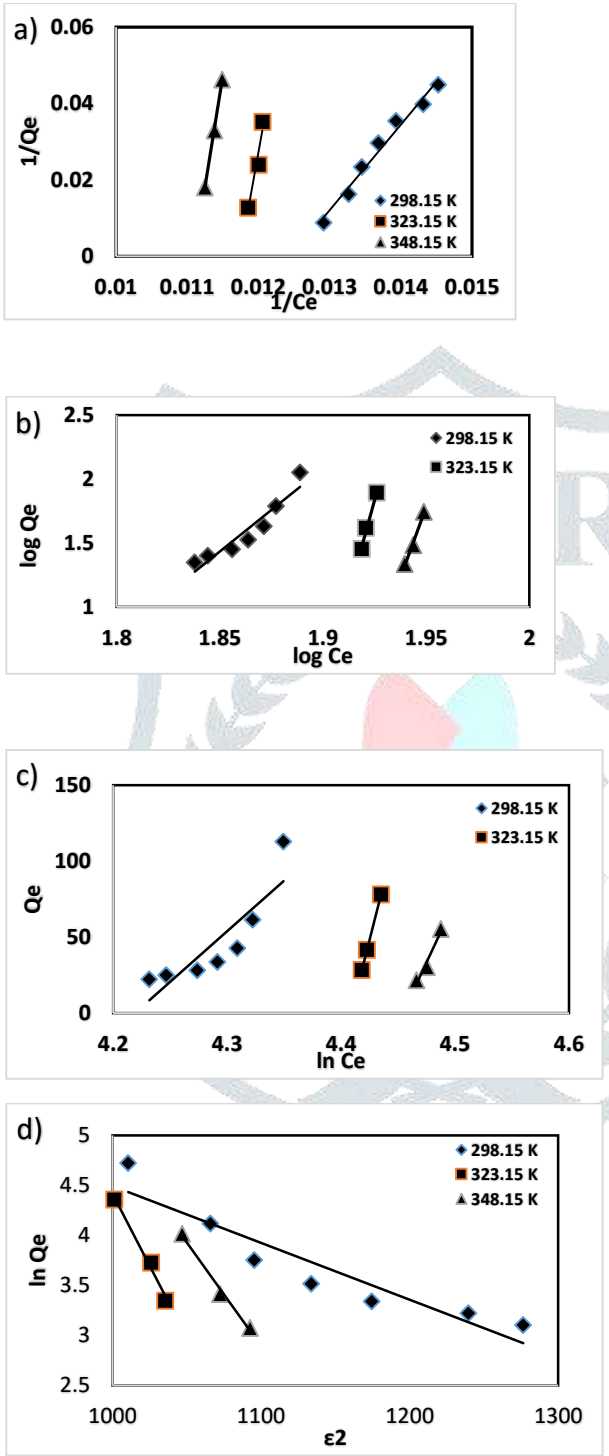

Fig.7: Different adsorption isotherms for adsorption of Rhodamine B dye on nosean at Different temperatures. (a) Langmuir adsorption isotherm, (b) Freundlich adsorption Isotherm, (c) Temkin adsorption Isotherm and (d) Dubinin-Radushkevich.

4.10 Adsorption thermodynamics

The thermodynamic parameters such as change in enthalpy (ΔH), entropy (ΔS) and Gibbs free energy (ΔG) for the adsorption process of Rhodamine B dye on nosean were evaluated using equation (13). The enthalpy change (ΔH) and entropy change (ΔS) are calculated from the slope and intercept of the plot of ln (K_a) versus 1/T (Fig. 8). The results of these thermodynamic calculations are presented in Table-5. The negative values for Gibbs free energy for adsorption of Rhodamine B

dye on nosean show that the adsorption process is spontaneous [62]. The overall adsorption process is found to exothermic in nature. $\Delta H = -12.6822$ kJmol^{-1}. Smaller absolute values of ΔH indicates that physical adsorption is the predominant mechanism in the adsorption process**.** This result supports the suggestion that the adsorption capacity of nosean decreases with increasing temperature. The ΔS values are negative and found to be -0.01955 kJ.mol^{-1}, for adsorption process of Rhodamine B dye and it confirms that the entropy decreases as a result of adsorption. This occurs as a result of redistribution of energy between the adsorbate and adsorbent. Before adsorption the Rhodamine B dye molecules near the surface of the adsorbent were in less ordered than in the subsequent adsorbed state. Negative value of ΔS indicates that the randomness decrease at the solid-solution interface during the process of adsorption [63]. Adsorption is occurring spontaneously at normal and it is more at normal room temperature and it decreases with temperature.

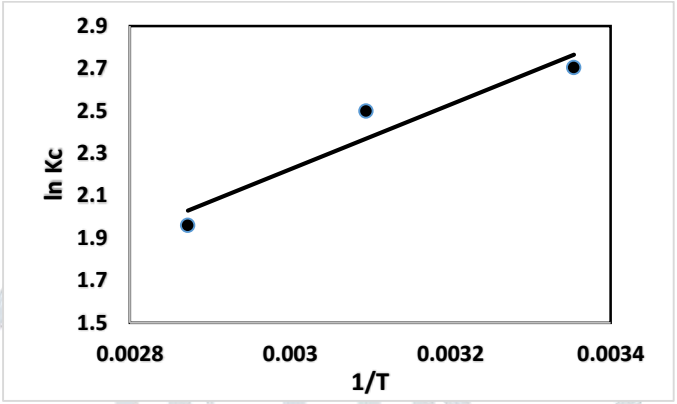

Fig. 8: Plot of ln Kc Vs 1/T for adsorption of Rhodamine B dye on nosean to determine ΔH (Enthalpy change) and ΔS (entropy change).

4.11 Adsorption kinetics

The rate of adsorption is an important parameter to understand the adsorption process. In order to study the adsorption of Rhodamine B dye onto hydrothermally synthesized nosean, pseudo-first-order, pseudo-second-order, intra-particle diffusion model and Bangham's equation were used by applying equation (15), (16), (17) and (18). Fig. 9 shows applicability of kinetic models for Rhodamine B dye and the data obtained is presented in Table-6.

It has been observed from the data, the correlation coefficient R^2 obtained from pseudo second order model were found to be larger 0.9597 than those found for pseudo first-order model (0.0656), intra-particle diffusion model (0.1178) and Bangham's model (0.2112).

Despite the Q_e (calculated) values in case of pseudo first order model are not matching with the Q_e (experimental) on the other hand Q_e (calculated) values are in good agreement with the Q_e (experimental) values in case of pseudo second order model. Thus adsorption of Rhodamine B dye onto nosean followed pseudo second order model well.

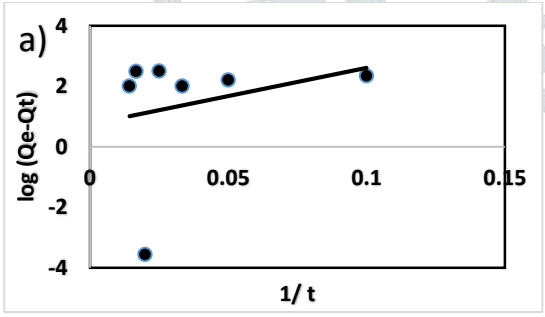

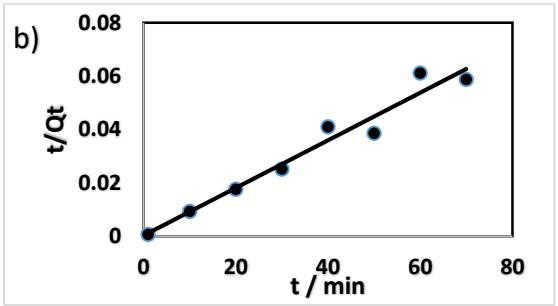

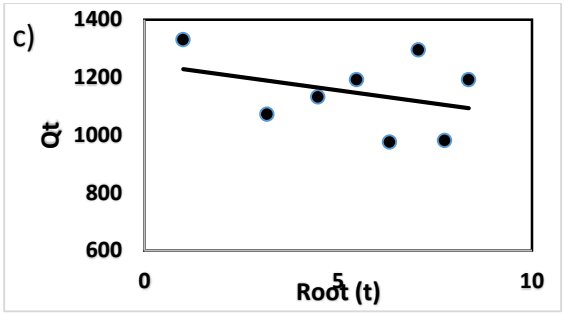

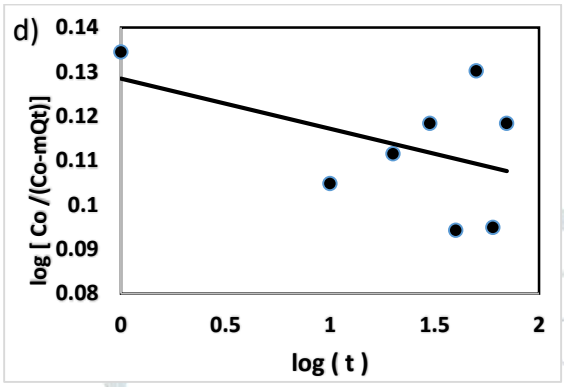

Fig.9: Different kinetic models for adsorption of Rhodamine B dye on nosean at room Temperatures, (a) Pseudo-first order, (b) Pseudo-second order, (c) Intra-particle diffusion model and (d) Bangham's model.

V. CONCLUSION

High content of Si and Al in coal fly ash makes it successfully possible to use it as a source material for the synthesis of alumino-silicate nosean. Hydrothermal synthesis of nosean required significantly less energy and reagent than traditional hydrothermal synthesis from pure reagents. Based on the isotherms, the specific surface area obtained from BET method is 62.024 $m^2.g^{-1}$ and BJH pore volume is 0.462 cc/g and radius Dv(r) = 87.341 ^{0}A.

First time we reports batch sorption study as a function of temperature for nosean with respect to Langmuir, Freundlich, Temkin and Dubinin-Radushkevich adsorption isotherms, out of which Langmuir's adsorption isotherm was found to have the highest regression value, hence the best fit. The Q_0 maximum monolayer coverage capacity ($mg.g^{-1}$) for Rhodamine B dye is found higher than any other adsorbent reported earlier by various researchers. The thermodynamic studies shows negative values of ΔG confirming, the feasibility of sorption process and also spontaneous nature. The negative and smaller values of ΔH and ΔS shows exothermic nature of the process and feasibility of sorption process and it is of physical nature. Negative value of ΔS indicates decrease in randomness at the solid-solution interface during the process of adsorption. The kinetic studies shows that sorption process is pseudo-second order.

VI. REFERENCES

1. Wang, S. and Zhu, Z. H. 2007. Effects of acidic treatment of activated carbons on dye adsorption. Dyes Pigments. 75: 306-314.
2. Errais, E., Duplay, J. and Darragi, F. 2010. Textile dye removal by natural clay – case study of Fouchana Tunisian clay. Environmental Technology. 31: 373-380.
3. Jain, R., Mathur, M., Sikarvar and Mittal, S. A. 2007. Removal of Hazardous dye Rhodamine B through photocatalytic and adsorption treatments. Journal of Environmental Management. 85: 956-964.
4. Martinez-Huitle, C. A., Brillas, E. 2009. Decontamination of wastewaters containing synthetic dyes by electrochemical methods: A general review. Applied Catalysis B. 87: 105-145.
5. Ledakowicz, S., Solecka, M. and Zylla, R. 2001. Biodegradation, decolourisation, and detoxification of textile wastewater enhanced by advanced oxidation process. Journal of Biotechnology. 89: 175- 184.
6. Salwa, M., Al-Rashed, Amani, A. and Al-Gaid. 2012. Kinetics and thermodynamic studies on adsorption behaviour of Rhodamine B dye on Duolite C-20 resin. Journal of Saudi Chemical Society. 16: 209-215.
7. Shen, K. and Gondal, M. A. 2013. Removal of Hazardous Rhodamine dye from water by adsorption onto exhausted coffee ground. Journal of Saudi Chemical Society. dx.doi. org / 10.1016 (2013).
8. Shah, J., Rasul Jan M., Haq, A. and Khan, Y. 2013. Removal of Rhodamine B from aqueous solutions and wastewater by walnut shells; kinetics, equilibrium and thermodynamic studies. Frontiers of Chemical Science and Engineering. 7 (4): 428-436.

9. Jain, R. Mathur, M., Sikarwar, S. and Nittal, A. 2007. Removal of hazardous due Rhodamine B through photocatalytic and adsorption treatment. Journal of Environmental Management. 85(4): 956-964.
10. Kooh, M. R. R., Dahri, M. K. and Lim, B. L. L. 2016. The removal of Rhodamine B dye from aqueous solution using casuarina equisetifolia needles as adsorbent. Congent Environmental Science. 2: 1140553.
11. Glasser, F. and Macphee, D. 1993. Immobilisation science of cement systems. MRS Bulletin. 18(3): 66-71.
12. Shigemoto, N., Hayashi, H. and Miyaura, K. 1993. Selective formation of Na-X, zeolite from coal fly ash by fusion with sodium hydroxide prior to hydrothermal reaction. Journal of Material Science. 28: 4781-478.
13. Amrhein, C., Haghnia G. H., Mosher, P. A., Gagajena, R. C., Amanios, T., and de la Torre, L. 1996. Synthesis and properties of zeolites from coal fly ash. Environmental Science and Technology. 30(3): 735-742.
14. Park, M., Choi, C., Lim, W., Kim, M., Choi, J. and Heo, N. 2000. Molten salt method for the synthesis of zeolitic materials: I zeolite formation in alkaline molten salt system, Microporous Mesoporous Materials. 37: 81-89.
15. Park, M., Choi, C., Lim, C., Kim, M., Choi, J. and Heo, N. 2000. Molten salt method for the synthesis of zeolitic materials: II Characterization of zeolitic materials. Microporous Mesoporous Mater. 37: 91-98.
16. Chareonpanich, M., Namto, T., Kongkachuichay, P. and Limtrakul, J. 2004. Synthesis of ZSM-5 zeolite from lignite fly ash and rice husk ash, Fuel Processing Technology. 85: 1623-1634.
17. Moriyama, R., Takedba, S., Onozakia, M.. Katayamaa, Y., Shiota, K. and Fukuda, T. 2005. Large scale synthesis of artificial zeolite from coal fly ash with a small charge of alkaline solution. Fuel. 84: 1455-1461.
18. Mimura, H., Yokota, K., Akiba, K. and Onodera, Y. 2001. Alkali Hydrothermal Synthesis of Zeolites from Coal Fly Ash and Their Uptake Properties of Caesium Ion, Journal of Nuclear Science and Technology. 38(9): 766-772.
19. Murayama, N., Yoshida, S., Takami, Y., Yamamoto, H. and Shibata, J. 2003. Simultaneous removal of NH^{4+} and PO_4^{3-} in aqueous solution and its mechanism by using zeolite synthesized from coal fly ash. Separation Science and Technology. 38(1): 113-130. DOI: 10.1081/SS-120016701.
20. Hiu, K. S., Chao, C.Y. H. and Kot, S. C. 2005. Removal of mixed metal ions in wastewater by zeolite 4A and residual product from recycled coal fly ash. Journal of Hazardous Materials. 127(1-3): 89-101.
21. Chen, J., Kong H., Wu, D., Hu, Z., Wang, Z. and Wang, Y. 2006, Removal of phosphate from aqueous solution by zeolite synthesized from fly ash. Journal of Colloid and Interface Science. 300: 491-497.
22. Wu, D., Zhang, B., Li, C., Zhang, Z. and Kong, H. 2006. Simultaneous removal of ammonia and phosphate by zeolite synthesized from fly ash as influenced by salt treatment, Journal of Colloid and Interface Science. 304: 300-306.
23. Zhang, B., Wu, D., Wang, C., He, S., Zhamg, Z. and Kong, H. 2007. Simultaneous removal of ammonia and phosphate by zeolite synthesized from fly ash as influenced by acid treatment. Journal of Environmental Science. 19(5): 540-545.
24. Qiu, W. and Zheng, Y. 2007. Arsenate removal from water by an alumina-modified zeolite recovered from fly ash, Journal of Hazardous Materials. 148(3): 721-726.
25. Somerset, V., Petrik, L. and Iwuoha, E. 2008. Alkaline hydrothermal conversion of fly ash precipitates into zeolites 3: The removal of lead and mercury from wastewater, Journal of Environmental Management. 87(1): 125-131.
26. Apiratikul, R. and P. Pavasant, P. 2008. Sorption of Cu^{2+}, Cd^{2+} and Pb^{2+} using modified zeolite from coal fly ash, Chem. Eng. J. 144 (2): 245-258.
27. Querol, X., Alastuey, A., Fernández-Turiel, J. and López-Soler, A.1995. Synthesis of zeolites by alkaline activation of ferro-aluminous fly ash. Fuel. 74(8): 1226-1231.
28. Lin, C. and Hsi, H.1995. Resource recovery of waste fly ash: synthesis of zeolite-like materials. Environmental Science and Technology. 29(4): 1109-1117. Doi:10.1021/es00004a033.
29. Kugbe, J., Matsue, N. and Henmi, T. 2009. Synthesis of Linde type A zeolite-goethite nanocomposite as an adsorbent for cationic and anionic pollutants. Journal of Hazardous Materials. 164: 929-935.
30. Berkgaut, V. and A. Singer, A. 1996. High capacity cation exchanger by hydrothermal zeolitization of coal fly ash. Applied Clay Science. 10: 369-378.
31. Querol, X., Alastuey, A., Lopez-Soler, A., Plana, F. 1997. Fast method for recycling fly ash: microwave assisted zeolite synthesis, Environmental Science and Technology. 31: 2527-2533. DOI**:** 10.1021/es960937t.
32. Steenbruggen, G. and Hollman, G. 1998. The synthesis of zeolites from fly ash and properties of the zeolite products, Journal of Geochemical Exploration. 62: 305-309.
33. Querol, X., Umana, J., Plana, F., Alastuey, A. and Lopez-Soler, A. 2001. A. Medinaceli, Synthesis of zeolites from fly ash at pilot plant scale. Examples of potential applications, Fuel. 80: 857-865.
34. Zhao, X., Lu, G. and Zhu, H. 1997. Effects of aging and seeding on the formation of zeolite Y from coal fly ash. Journal of Porous Materials. 4(4): 245-251.
35. Chang, H. and Shih, W. 1998. A General Method for the Conversion of Fly Ash into Zeolites as Ion Exchangers for Cesium. Industrial and Engineering Chemistry Research. 37(1): 71-78. DOI: 10.1021/ie970362o.
36. Hollman, G., Steenbruggen, G. and Janseen-Jurkovicova, M. 1999. A two-step process for synthesis of zeolites from coal fly ash. Fuel. 78(10): 1225-1230.
37. Wang, C., Li, J., Sun, X., Wang, L. and Sun, X. 2009. Evaluation of zeolites synthesized from coal fly ash as a potential adsorbent for wastewater containing heavy metals. Journal of Environmental Science. 21(1): 127-136.
38. Jha, V. K., Nagae, M., Matsuda, M. and Miyake, M.2009. Zeolite formation from coal fly ash and heavy metal ion removal characteristics of thus obtained zeolite X in multi-metal system. Journal of Environmental Management. 90(8): 2507-2514.
39. Vanderborght, B. M., Van Griekenm, R. E. 1977. Enrichment of trace metals in water by adsorption on activated carbon. Analytical Chemistry. 49(2): 311-316. DOI: 10.1021 /ac50010 a032.

40. Hall, K. R., Eagleton, L. C., Acrivos, A. and Vermeulen, T. 1966. Pore- and Solid Diffusion Kinetics in Fixed-Bed Adsoprtion under Constant-Pattern Conditions. Industrial and Engineering Chemistry Fundamentals. 5(2): 212-223.
41. Langmuir, I. 1918. The adsorption of gases on plane surface of glass, mica and platinum. Journal of American Chemical Society. 40(9): 1361-1403. DOI**:** 10.1021/ja02242a004.
42. Webber, T. W. and Chakravorti, R. K. 1974. Pore and Solid Diffusion Models for fixed bed absorbers. American Institute of Chemical Engineers Journal. 20: 228-238.
43. Voudrias, E., Fytianos, K. and Bozani, E. 2002. Sorption Description Isotherms of Dyes from aqueous solutions and Waste Water with Different Sorbent materials, Global Nest. 4(1)*:* 75-83.
44. Venkata Mohan, S. and Karthikeyan, J. 1997. Removal of lignin and tannin colour form aqueous solution by adsorption onto activated charcoal. Environmental Pollution. 97 (1997) 183-187.
45. Goldberg, S. 2005. Equations and Models Describing Adsorption Processes in Soils, Chemical Processes in Soils. pp.489. Published by: Soil Science Society of America, Inc. Madison, Wisconsin, USA.
46. Temkin, M. I. and Pyzhev, V. 1940. Kinetics of Ammonia Synthesis on Promoted Iron Catalyst, Acta Physico-Chimica USSR. 12: 217-222.
47. Aharoni, C. and Ungarish, M. 1977. Kinetics of activated chemisorption. Part-2. Theoretical models, Journal of Chemical Society Faraday Transactions. 73: 456- 464.
48. Gunay, A., Arslankaya, E. and Tosun,I. 2007. Lead removal from aqueous solution by natural and pre-treated clinoptilolite: Adsorption equilibrium and kinetics. Journal of Hazardous Materials. 146: 362-371.
49. Dabrowski, A. 2001. Adsorption- from theory to practice, Advances in Colloid and Interface Science. 93: 135-224.
50. Lagergren, S. 1898. About the theory of so- called adsorption of soluble substances, Kunglica Svenska Vetenskapsakademiens. Handlingar. 24(4): 1-39.
51. Ho, Y. S. and McKay, G. 1999. Pseudo-second-order model for sorption processes, Process Biochemistry. 34(5): 451-465.
52. Khaled, A., Nemr, A. E., El-Sikaily and Abdelwahab, A. O. 2009. Removal of Direct N Blue-106 from artificial textile dye effluent using activated carbon from orange peel: Adsorption isotherm and kinetics studies. Journal of Hazard. Material. 165: 100-110.
53. Mane, V. S., Mall, I. D. and Srivastava, V. C. 2007. Kinetic and equilibrium isotherm studies for the adsorptive removal of Brilliant Green dye from aqueous solution by rice husk ash, Journal of Environmental Management. 84(4): 390-400.
54. Vimonses, V., Lei, S., Jin, B.,. Chow, C.W. K and Saint, C. 2009. Adsorption of Congo red by three Australian kaolin, Applied Clay Science. 43: 465-472.
55. Bilgili, M. S. 2006. Adsorption of 4-chlorophenol from aqueous solutions by Xad-4 resin: Isotherm, kinetic, and thermodynamic analysis, Journal of Hazardous Matter. B 137: 157-164.
56. Aharoni, C., Sideman, S. and Hoffer, E. 1979. Adsorption of phosphate ion by collodion coated alumina, Journal of Chemical Technology and Biotechnology 29(7): 404 -412.
57. Khare, P. and Baruah, B. P. 2010. Chemometric analysis of trace elements distribution in raw and thermally treated sulphur coals. Fuel Processing Technology. 91(11): 1691-1701.
58. Periasamy, A., Muruganand, S. and Palaniswamy, M. 2009. Vibrational studies of Na_2SO_4, K_2SO_4, $NaHSO_4$ and $KHSO_4$ crystals. Rasayan Journal of Chemistry. 2(4): 981-989.
59. Shah, J., Jan, M. R., Haq, A. and Khan, Y. 2013. Removal of Rhodamine B from aqueous solution and waste water by Walnut Shells: Kinetics, equilibrium and thermodynamics studies. Frontiers of Chemical Science and Engineering. **7**(4): 428-436.
60. Khan, T. A. Sharma, S. and Ali, I. 2011. Adsorption of Rhodamine B dye from aqueous solution onto acid activated mango (Magnifera indica) leaf powder: Equilibrium, kinetic and thermodynamic studies, Journal of Toxicology and Environmental Health Sciences 3(10): 286-297.
61. Yong, Q. Z. and Zaini, M. A. A. 2016. Adsorption of Rhodamine B by Palm Kernel Shell Adsorbents, Journal of Engineering and Technology. 7(2): 1-16.
62. Horsfall, M., Spiff, A. I. and Abia, A. A. 2004. Studies on the influence of mercaptoacetic acid (MAA) modification of cassava (Manihot sculenta crantz) waste Biomass on adsorption of Cu^{2+} and Cd^{2+} from aqueous solution, Bull Korean Chem. Soc. 25(7): 969-976.
63. Bao, W. Zou, H. Gan, S. Xu, X. Ji, G. and Zheng, K. 2013. Adsorption of heavy metal ions from aqueous solutions by zeolite based on oil shale ash: Kinetic and equilibrium studies, Chemical Research in Chinese Universities. 29: 126-13.